

Supporting Information

for

“A retrospective analysis of mid-summer hypoxic area and volume in the northern Gulf of Mexico, 1985-2011”

by

Daniel R. Obenour*, Donald Scavia, Nancy N. Rabalais, R. Eugene Turner, and Anna M. Michalak

consisting of

7 sections with 16 figures and 4 tables in 17 pages.

*corresponding author, obenour@umich.edu

S1. Instrument adjustment

Using data from sampling events where both the rosette and handheld samplers were deployed, we developed relationships between the hypoxic conditions (BWDO and hypoxic thickness) derived from the synthesized data (both instruments) and the hypoxic conditions derived from rosette-only data. Figure S1 presents BWDO values derived from the synthesized data (S_{BO}) versus BWDO values from the rosette-only data (R_{BO}). We divided the data into two different categories (blue and red, Figure S1), where the blue data meet the following criterion:

$$S_{BO} - R_{BO} > 2\sigma_{\epsilon} \quad \text{eq S1}$$

where σ_{ϵ} is the standard deviation of the stochasticity that is not spatially correlated (i.e. microvariability), as described in the primary text. For the blue data, the relationship between S_{BO} and R_{BO} can be represented approximately using a simple linear regression with normally distributed residuals (ϵ):

$$\hat{S}_{BO,blue} = 0.973R_{BO,blue} + \epsilon \quad \text{eq S2}$$

The remaining (red) data can be modeled as a uniform distribution between zero and the threshold criterion used in eq S1:

$$\hat{S}_{BO,red} \sim U(0, [R_{BO,blue} - 2\sigma_{\epsilon}]) \quad \text{eq S3}$$

Using these relationships, we can simulate values of S_{BO} for rosette-only sampling events. (Each conditional realization is assigned a unique set of simulated values.) For R_{BO} less than $2\sigma_{\epsilon}$ mg L^{-1} , eq S2 always applies. For R_{BO} greater than $2\sigma_{\epsilon}$ mg L^{-1} , eq S2 is applied at an 88.9% probability and eq S3 at an 11.1% probability. These percentages reflect the actual partitioning of the data as presented in Figure S1. From a physical perspective, application of eq S3 represents situations where there is a thin, high-density, bottom layer that is not reached by the rosette. Conversely, the application of eq S2 implies that the rosette did reach the bottom-most layer of water. When performing simulations, we do not sample from the error term (ϵ) in eq S2, as this variability is expected to be primarily reflective of the microvariability already accounted for within the covariance model.

For hypoxic thickness, the relationship between the synthesized and rosette-only data is somewhat simpler (Figure S2). Here, the relationship between synthesized thickness (S_{Th}) and rosette thickness (R_{Th}) can be approximately modeled using a simple linear regression with normally distributed residuals (the units of the equation are meters):

$$\hat{S}_{Th} = R_{Th} + 0.82 + \epsilon \quad \text{where ... } \epsilon \sim N(0,0.36) \quad \text{eq S4}$$

When performing simulations, we do sample from the error term (ϵ) of eq S4, as this error is expected to be primarily reflective of the variability in the maximum rosette sampling depth, rather than the natural variability in the thickness of the hypoxic layer. For observations that are not hypoxic based on the rosette measured BWDO, but become hypoxic when performing the instrument adjustment for BWDO ($R_{BO} > 2 \text{ mg L}^{-1}$ and $\hat{S}_{BO} < 2 \text{ mg L}^{-1}$), we multiply \hat{S}_{Th} (which

is $0.82 + \epsilon$ in this case) by a sample from a standard uniform distribution because it is unclear what portion of the offset is hypoxic. Although more realistic, this additional step has a negligible impact on results.

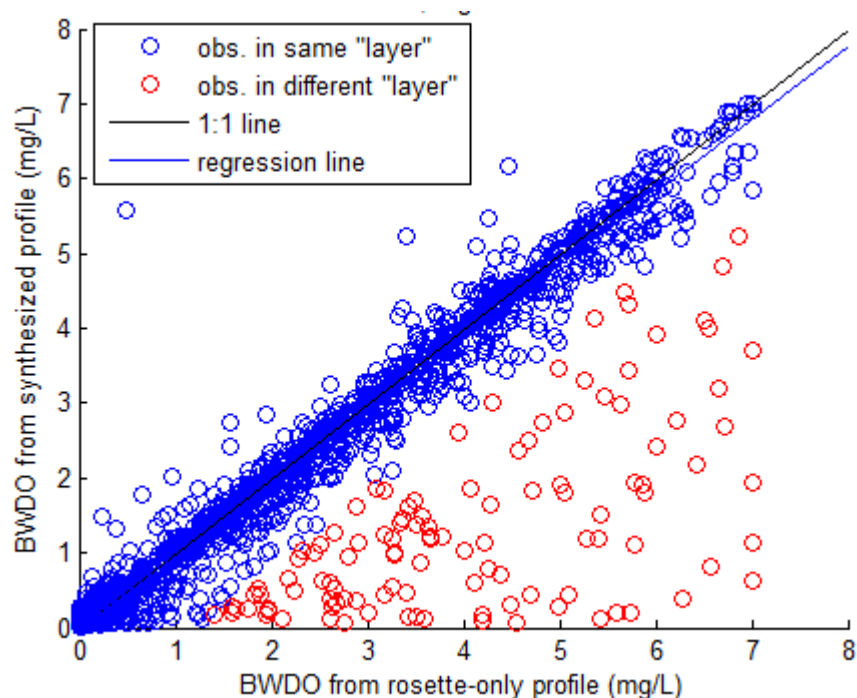


Figure S1: BWDO from synthesized data (S_{BO}) vs. BWDO from rosette instrument only (R_{BO})

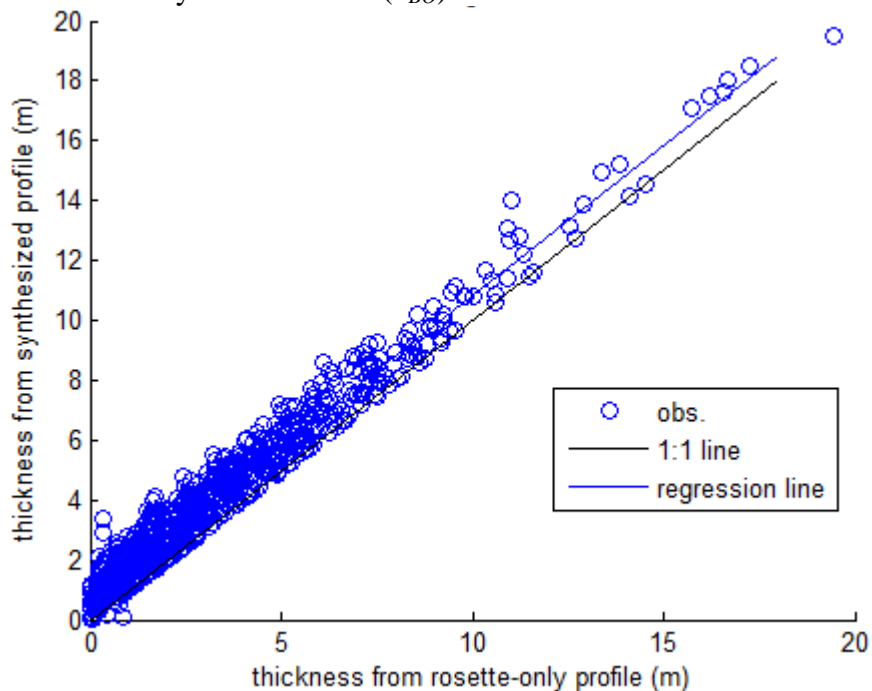


Figure S2: Hypoxic thickness from synthesized data (S_{Th}) vs. hypoxic thickness from rosette instrument (R_{Th})

As described in the primary text, in 1991 a larger bias adjustment was required for the first 38 sampling events because the ship's fathometer was not functioning correctly, causing the rosette sampler to be lowered 1.5 meters less than it would have been otherwise. The same type of adjustment was performed for these events, using eq's S5, S6 and S7, which are analogous to eq's S2, S3, and S4, respectively. For $R_{1.5,BO}$ greater than $2\sigma_\epsilon$ mg L⁻¹, eq S2 is applied at an 67.5% probability and eq S3 at an 32.5% probability.

$$\hat{S}_{BO,blue} = -0.163 + 0.967R_{1.5,BO,blue} + \epsilon \quad \text{eq S5}$$

$$\hat{S}_{BO,red} \sim U(0, (R_{1.5,BO,blue} - 2\sigma_\epsilon)) \quad \text{eq S6}$$

$$\hat{S}_{Th} = R_{1.5,Th} + 2.3 + \epsilon \quad \text{where ... } \epsilon \sim N(0,0.39) \quad \text{eq S7}$$

S2. Test of linearity assumption for deterministic trends

In Figures S3 and S4, we plot the residuals (stochastic portion) of the UK models for BWDO and hypoxic fraction, respectively, versus each of the trend variables used in these models. Because the residuals are generally evenly distributed around zero throughout the ranges of the trend variables, the linear model formulation appears reasonable. Note that the models do include nonlinear transformations of the trend variables (i.e. depth-squared) but they are incorporated within a linear modeling framework.

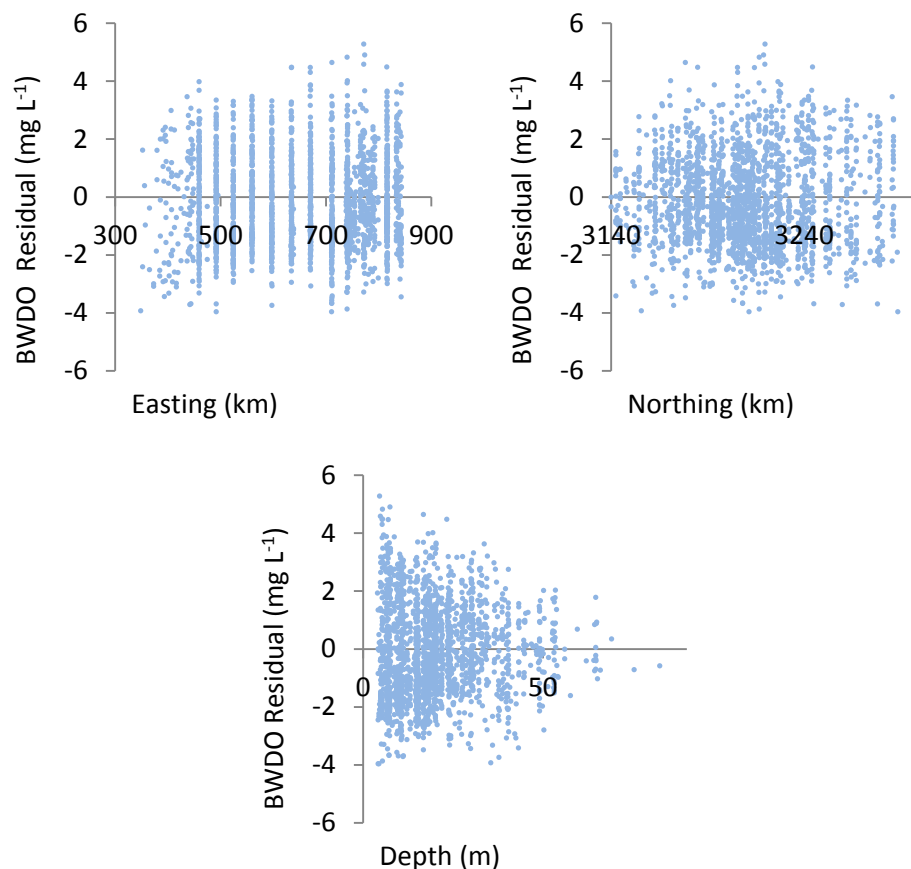


Figure S3: BWDO residuals (stochastic portion of UK model) vs. covariates

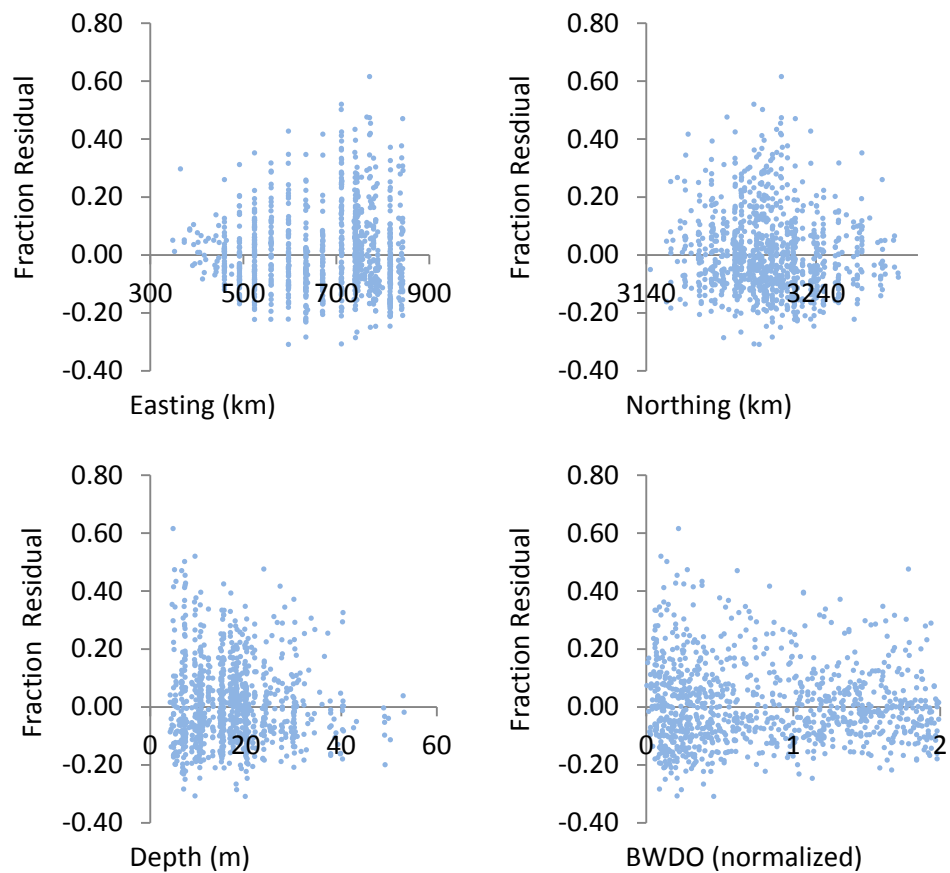


Figure S4: BWHF residuals (stochastic portion of UK model) vs. covariates

S3. Intercept values for BWDO and BWHF models

Table S1: Annual, cruise-specific intercept values for BWDO and BWHF models

year	BWDO (mg L ⁻¹)	BWHF (-)
1985	2.43	0.188
1986	2.71	0.179
1987	3.13	0.161
1988	5.40	0.096
1989	3.30	0.111
1990	2.84	0.164
1991	2.71	0.145
1992	2.76	0.141
1993	1.91	0.200
1994	2.30	0.213
1995	1.94	0.184
1996	1.65	0.209
1997	2.03	0.189
1998	2.71	0.180
1999	1.82	0.306
2000	4.19	0.240
2001	2.13	0.221
2002	1.97	0.188
2003	3.63	0.149
2004	2.22	0.322
2005	2.99	0.229
2006	2.51	0.217
2007	2.01	0.292
2008	1.84	0.262
2009	3.82	0.296
2010	2.10	0.269
2011	2.39	0.202

S4. Tabulated bottom layer hypoxic area and volume estimates

Table S2 tabulates the geostatistical extent estimates presented graphically in Figure 3 of the main text (based on CRs from UK model formulation)

Table S2: Bottom layer hypoxic areas and volume results

Year	Area (1000 km ²)				Volume (km ³)			
	mean	median	2.5 perc	97.5 perc	mean	median	2.5 perc	97.5 perc
1985	14.3	14.4	10.6	18.0	53.6	52.2	32.8	83.4
1986	12.7	12.5	9.4	17.0	39.0	37.5	24.3	61.7
1987	9.8	9.6	6.8	14.3	24.2	22.5	12.1	46.7
1988	0.7	0.6	0.2	1.7	1.3	0.8	0.0	5.3
1989	10.4	9.7	4.7	20.6	28.4	24.0	10.2	69.6
1990	15.0	14.6	10.5	21.6	59.3	57.2	37.1	94.7
1991	17.9	17.6	13.4	23.9	70.0	67.4	44.3	112.9
1992	11.6	11.3	8.7	16.1	33.7	32.5	22.0	54.2
1993	22.7	22.4	18.6	28.7	99.5	97.0	71.2	139.2
1994	16.6	16.4	12.9	21.4	73.8	72.4	51.2	103.9
1995	21.3	20.9	17.0	27.2	66.3	64.1	44.0	105.0
1996	23.2	22.9	18.5	29.6	92.9	89.5	64.3	139.0
1997	18.2	17.9	14.7	22.9	54.8	52.1	36.8	88.2
1998	11.1	11.0	9.2	13.2	54.9	53.6	38.5	74.8
1999	21.2	21.0	16.8	27.1	111.3	108.9	77.2	158.6
2000	3.8	3.7	2.7	5.2	15.0	14.4	8.5	24.2
2001	20.1	19.9	16.8	24.5	73.0	71.6	52.2	101.9
2002	21.7	21.6	18.5	25.7	67.6	65.6	48.3	94.3
2003	5.5	5.5	4.1	7.3	11.3	11.0	6.1	18.5
2004	15.7	15.4	12.5	20.0	83.6	80.0	54.2	131.6
2005	10.2	10.2	8.1	13.1	30.7	29.4	19.7	47.9
2006	15.6	15.5	12.5	19.9	62.6	60.9	42.9	90.9
2007	20.6	20.6	17.0	25.1	107.0	104.9	75.1	153.4
2008	22.3	22.3	18.8	26.2	137.5	135.2	101.3	185.5
2009	7.1	7.0	5.7	8.5	44.3	43.6	32.5	61.3
2010	15.6	15.5	12.1	19.4	65.6	63.9	42.8	102.1
2011	17.1	17.1	14.4	19.9	62.6	61.5	47.0	83.1
average	14.9	14.7	11.7	19.2	60.1	58.3	40.6	90.1

S5. Results maps (based on CRs from UK model formulation)

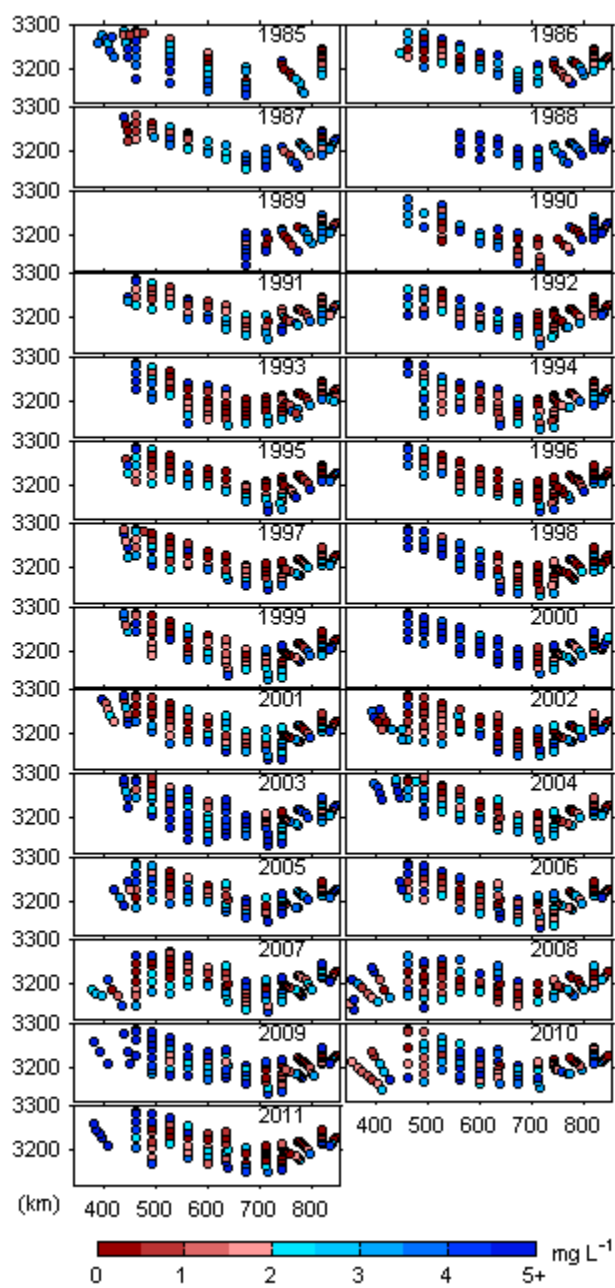


Figure S5: Observed BWDO concentration

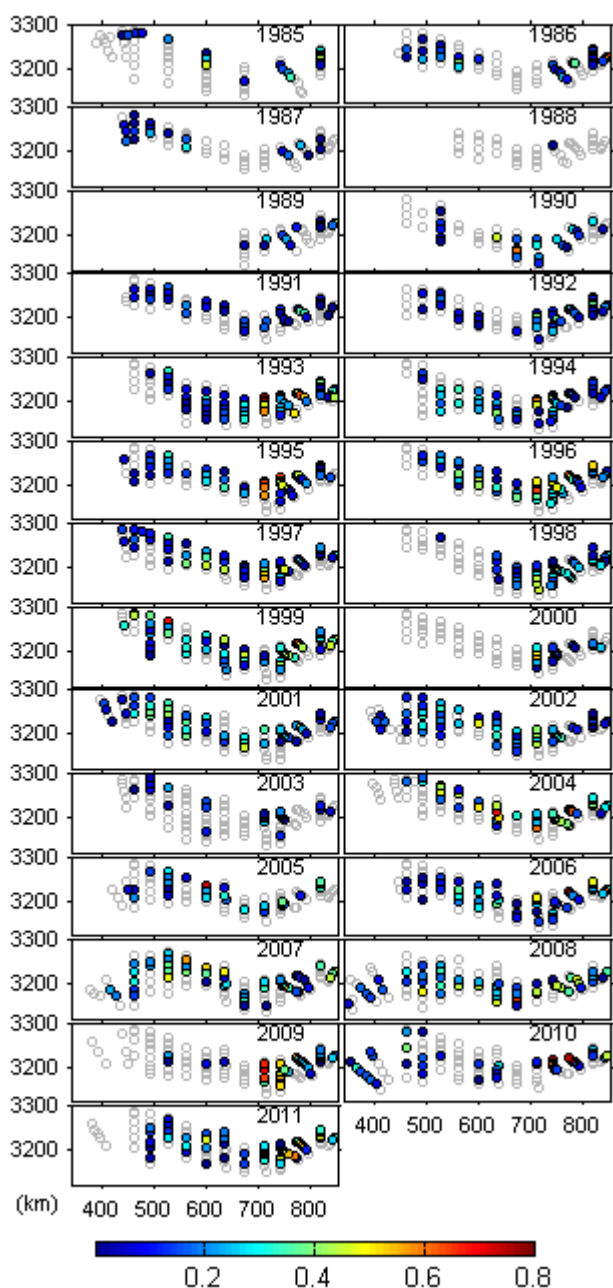


Figure S6: Observed BWHF

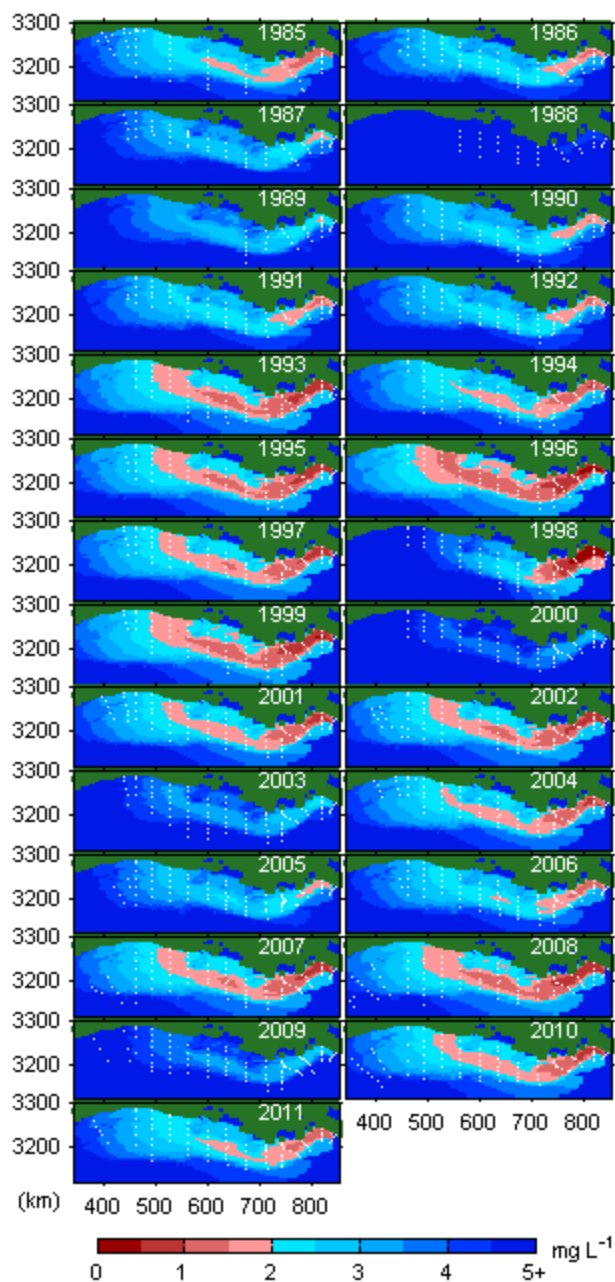


Figure S7: BWDO deterministic trend (note that the spatial pattern is the same for all years, except 1998)

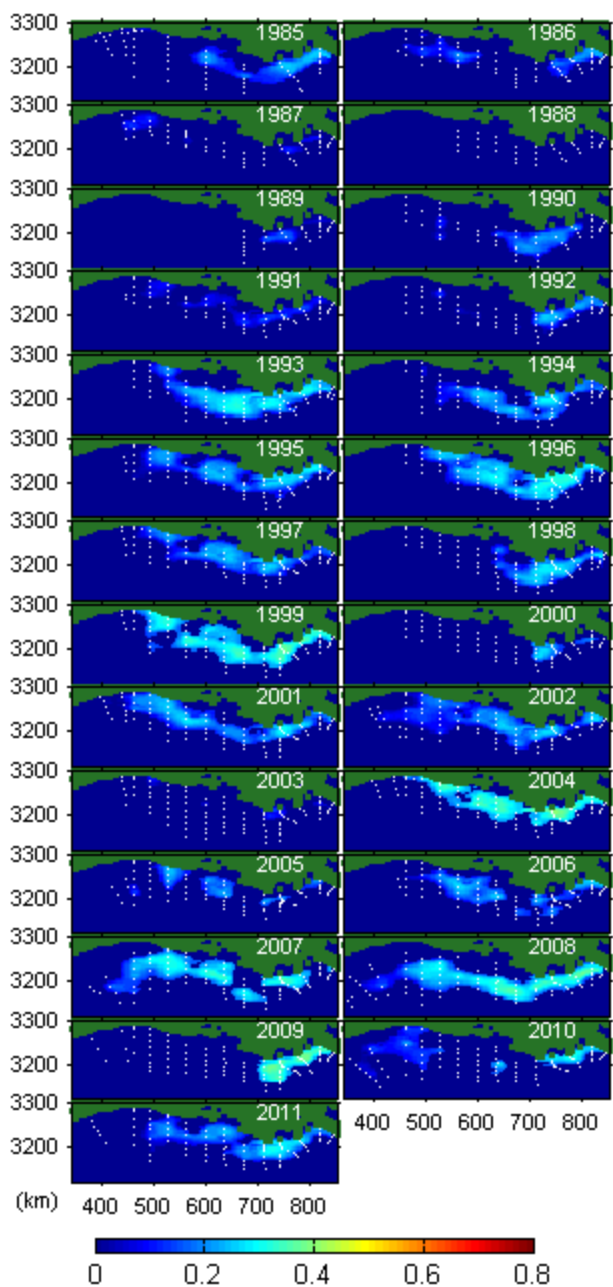


Figure S8: BWHF deterministic trend (using kriged BWDO as a trend variable)

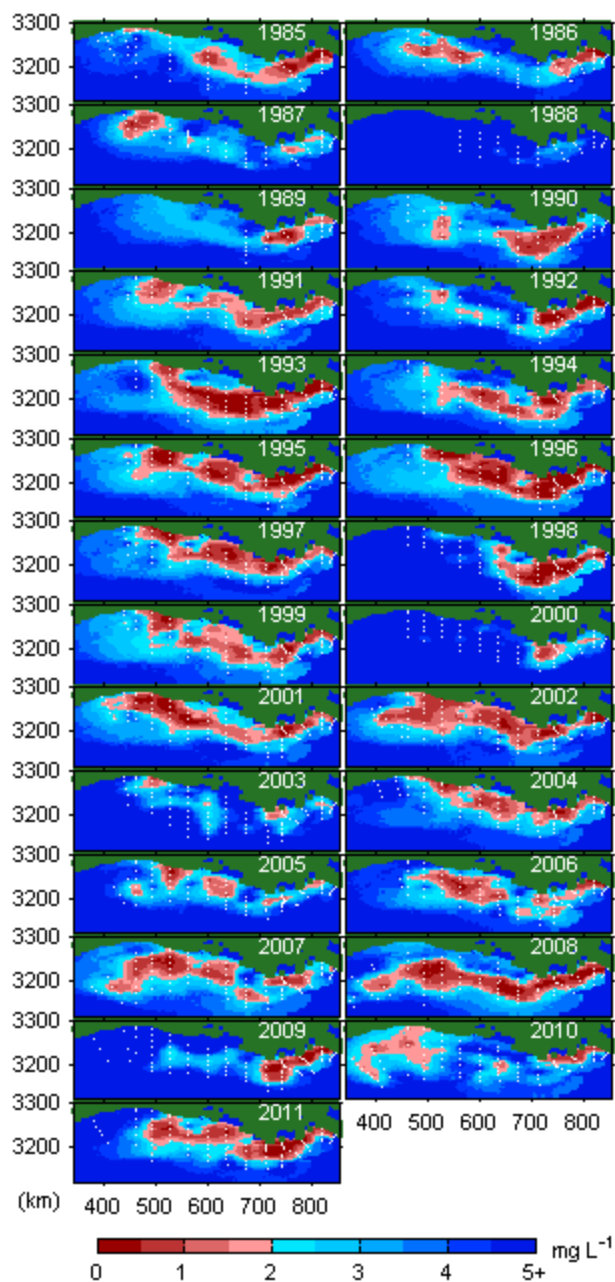


Figure S9: Median BWDO concentration from CR (note that these results are the same as kriged results, except they also include the instrument bias adjustment, which was implemented through the CR process)

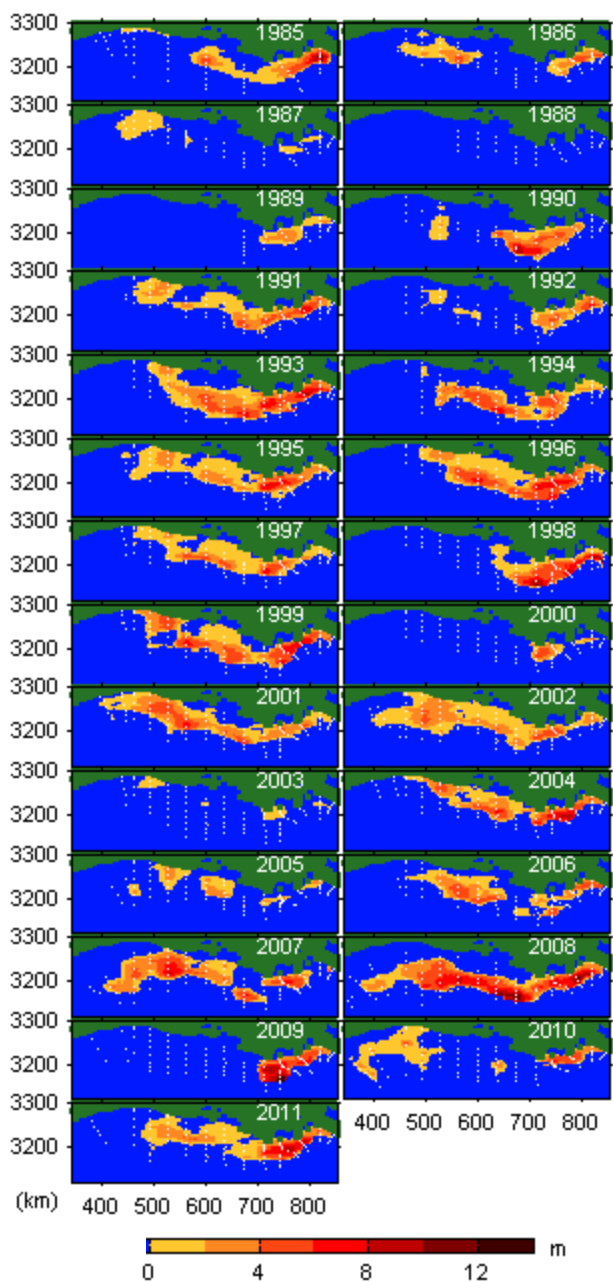


Figure S10: Median BW hypoxic thickness from CR

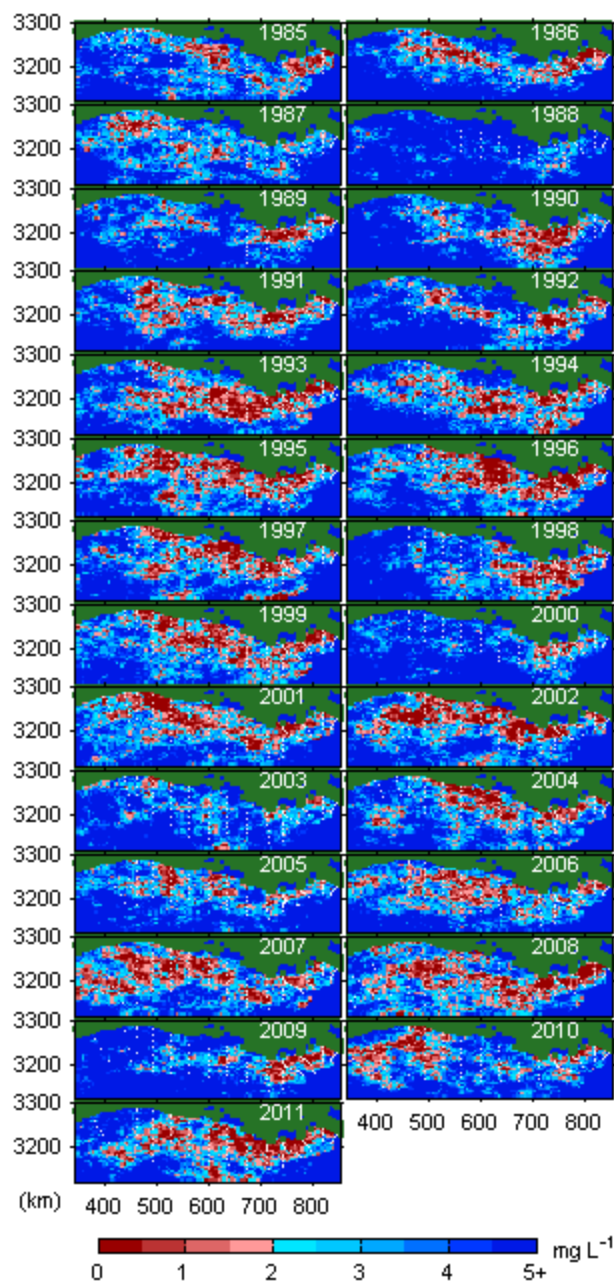


Figure S11: Example conditional realizations of BWDO concentration

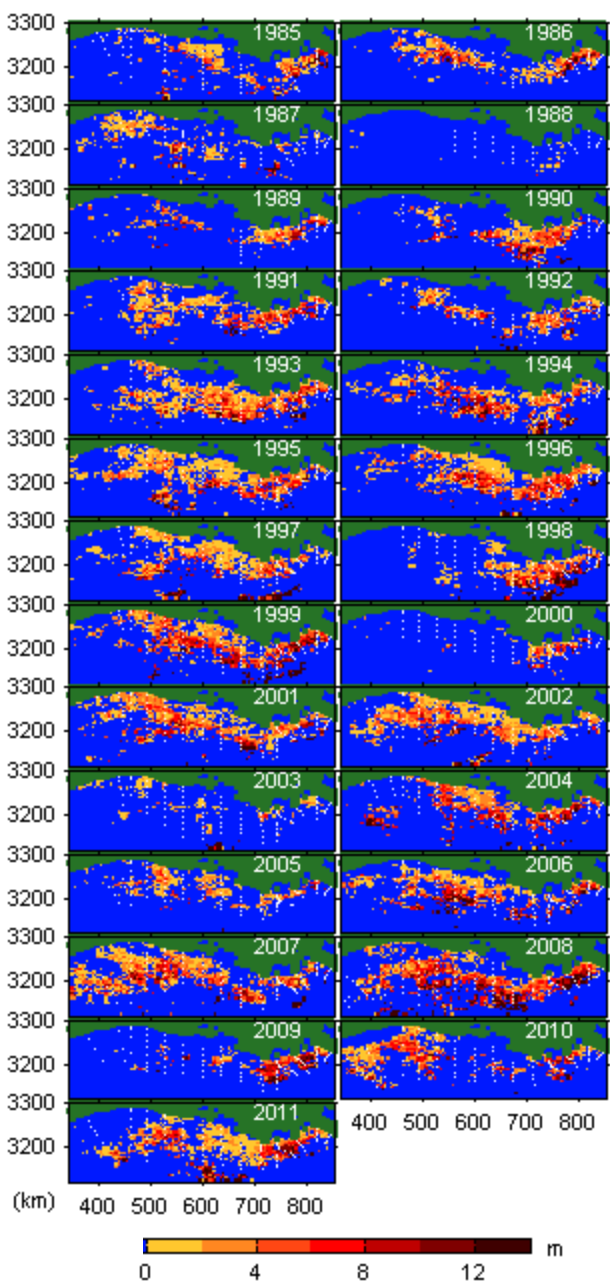


Figure S12: Example conditional realizations of BW hypoxic thickness

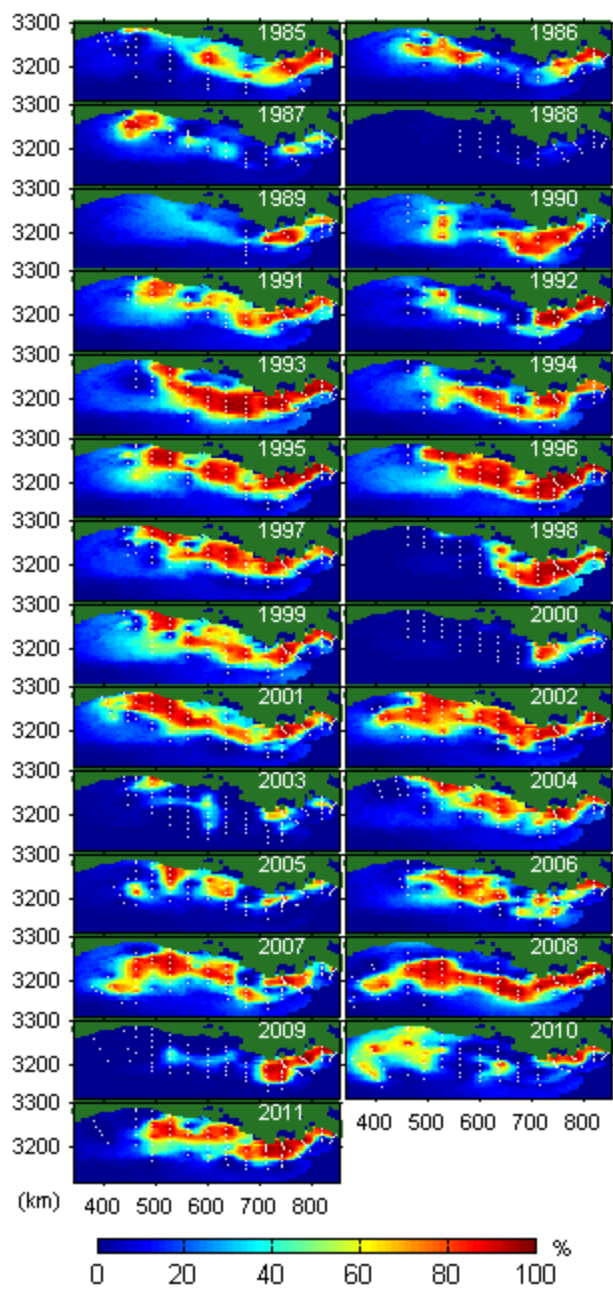


Figure S13: Probability of hypoxia

S6. Comparison of bottom layer extent results using different methods

The hypoxic extent can be determined using a variety of different interpolation and simulation-based methods. Figure S14 compares the preferred area estimates (CRs from UK, with instrument adjustment, Table S2) to areas inferred from less-optimal methods. This comparison includes interpolation ('kriged') estimates, which are consistently lower than the results determined from other methods, as described in the main text.

This comparison also includes estimates developed using CRs from an OK formulation (without trend variables). The "OK" estimates have average confidence intervals more than twice as wide as those from UK; and the OK hypoxic area and volume estimates are 53% and 121% greater than the UK estimates, respectively. OK tends to over-estimate the extent of hypoxia outside of the sampling cruise envelope, because unlike UK, OK does not use trend variables to represent large-scale spatial patterns in DO and hypoxic fraction. These trends (Figures S7 and S8) generally indicate that conditions become less hypoxic as one moves away from the most intensively sampled areas of the shelf.

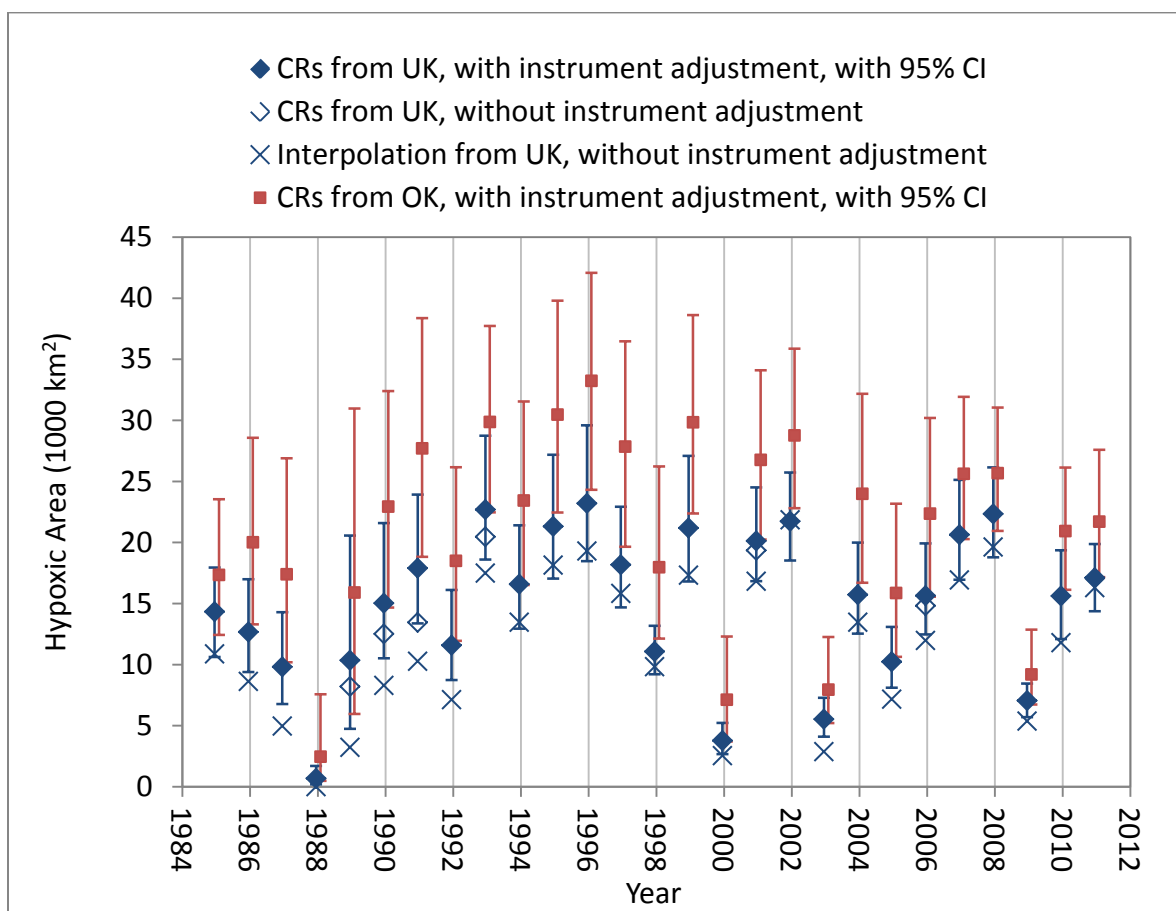


Figure S14: Hypoxic extent estimates developed using different methods

S7. Models for MinDO and THF

In the main text, we describe the models for BWDO and BWHF, which yield the area and volume of the hypoxic bottom layer. However, models can also be developed for the minimum dissolved oxygen (MinDO) and total hypoxic fraction (THF) which yield the total hypoxic area and volume. These models account for layers of hypoxia existing higher (i.e., suspended) in the water column. The parameterization and results of these models are provided below. Table S3 corresponds to Table 1 in the primary text. Table S4 presents the total hypoxic area and volume results (CR+UK methodology), corresponding to Table S2. Figures S15 and S16 present maps of expected MinDO and total hypoxic thickness, corresponding to Figure S9 and S10.

In general, the results for total hypoxic area and volume are similar to the results for bottom layer hypoxic area and volume (as presented in the main text). On average, the total hypoxic area is 14% larger than the bottom layer hypoxic area, and the two sets of estimates are highly correlated ($r^2=0.97$). Similarly, the total hypoxic volume is 18% larger than the bottom layer hypoxic volume, on average, and they are also highly correlated ($r^2=0.97$). This indicates that the traditionally reported bottom layer hypoxic extent is also proportionally representative of the total hypoxic extent.

Table S3: MinDO and THF model parameters

Variable	MinDO (mg L^{-1})		THF	
	β	σ_β	β	σ_β
E	-0.74	0.09		n.s.
E ²	0.32	0.07		n.s.
N	-0.45	0.09	-0.0054	0.007
N ²			-0.0164	0.006
D	-2.45	0.18		n.a.
D ²	2.39	0.16		n.a.
O		n.a.	-0.080	0.004
O ²		n.a.		n.s.
c.s. E 1998	-1.29	0.43		n.s.
c.s. E 2010	1.04	0.33		n.s.

c.s.=cruise specific, n.s. = not selected, n.a. = not available

Supporting Information for: A retrospective analysis of mid-summer hypoxic area and volume in the northern Gulf of Mexico, 1985-2011

Table S4: Total hypoxic area and hypoxic volume results*

Year	Area (1000 km ²)				Volume (km ³)			
	mean	median	2.5 perc	97.5 perc	mean	median	2.5 perc	97.5 perc
1985	15.8	15.8	12.3	19.6	63.7	62.5	39.5	92.9
1986	14.6	14.4	11.1	19.0	45.1	43.3	27.9	71.9
1987	10.3	10.1	7.1	14.3	25.4	23.9	12.5	46.4
1988	0.6	0.6	0.2	1.4	1.2	0.8	0.0	4.5
1989	13.7	13.1	6.5	23.6	41.6	37.1	15.4	92.2
1990	15.8	15.6	11.7	21.3	61.6	59.3	39.3	95.7
1991	21.1	20.9	16.1	27.6	86.0	82.7	52.6	139.2
1992	12.7	12.4	9.8	16.9	42.0	40.4	27.8	66.0
1993	24.4	24.2	19.9	30.5	112.6	110.1	82.5	160.0
1994	18.4	18.2	14.8	22.9	89.4	87.6	62.1	130.6
1995	25.3	25.2	20.5	31.3	88.1	85.6	58.4	131.6
1996	25.0	24.8	20.0	31.6	109.3	105.2	74.2	163.2
1997	21.2	20.9	17.3	26.5	71.0	67.9	45.9	114.8
1998	11.7	11.7	9.9	13.8	58.6	57.4	42.6	81.8
1999	28.2	27.9	23.0	34.6	140.4	138.3	96.4	197.5
2000	3.9	3.8	2.8	5.3	15.9	15.3	9.1	26.5
2001	23.9	23.8	20.0	29.0	88.8	86.9	64.2	125.8
2002	24.3	24.1	20.7	28.6	74.7	72.5	53.3	105.0
2003	6.6	6.6	5.1	8.5	14.2	13.4	7.6	24.5
2004	19.7	19.4	15.8	24.9	107.6	104.5	71.9	161.7
2005	10.8	10.6	8.5	13.5	34.3	33.0	21.4	54.5
2006	16.6	16.4	13.6	20.6	69.1	67.1	47.6	102.9
2007	23.3	23.2	19.3	27.8	123.6	120.9	88.8	173.8
2008	26.1	26.2	22.4	30.3	142.8	140.6	110.2	190.8
2009	8.9	8.9	7.4	10.7	51.9	50.9	38.7	71.9
2010	20.2	20.1	16.2	24.4	78.9	77.6	54.8	110.5
2011	20.7	20.6	17.8	24.0	82.1	81.1	61.6	110.4
average	17.2	17.0	13.7	21.6	71.1	69.1	48.4	105.4

*Note that these results are for total hypoxic area and volume. They are different from the bottom-layer results (Table S2) which were the focus of the primary text.

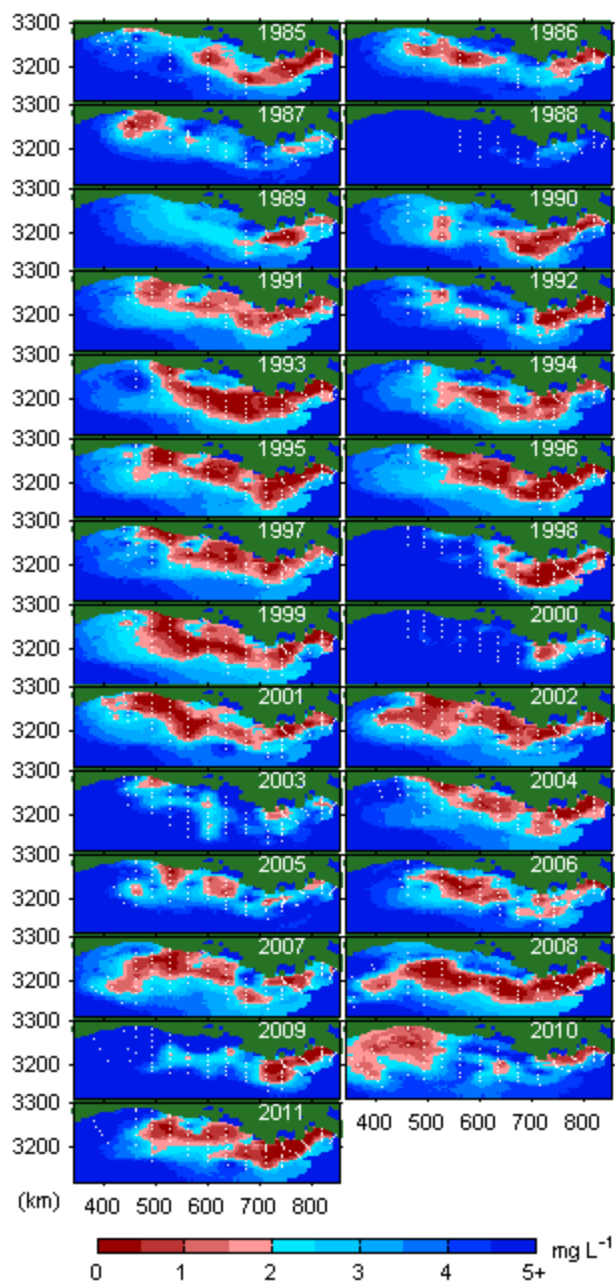


Figure S15: Median MinDO concentration

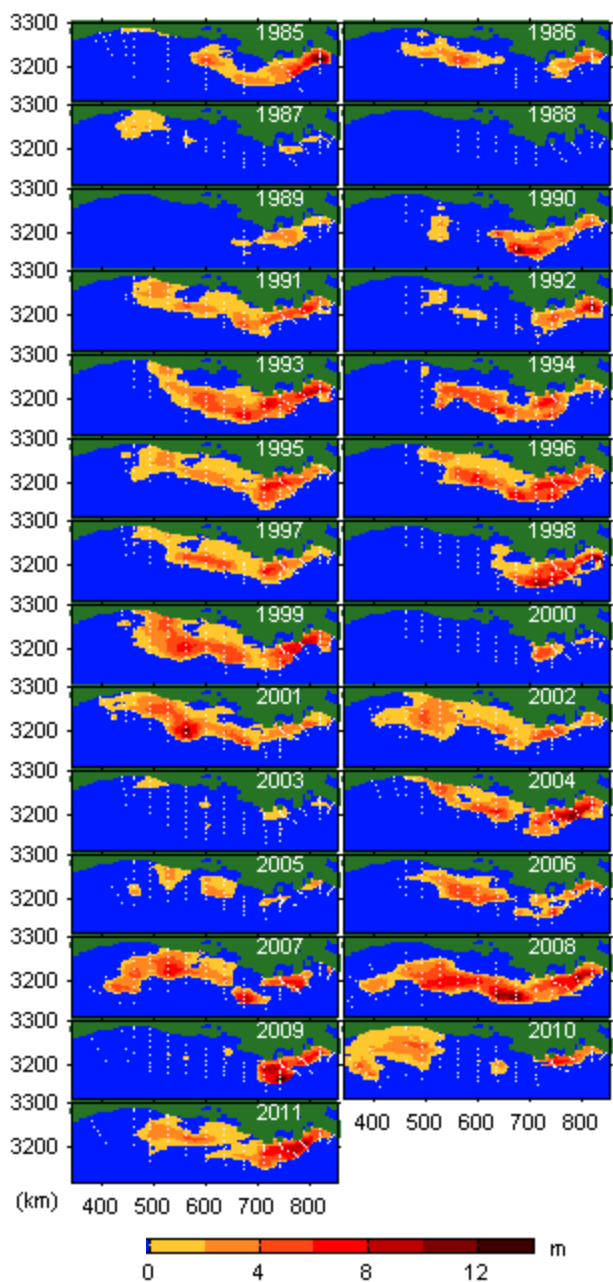


Figure S16: Median total hypoxic thickness